On the Throughput Limit of Multi-Hop Wireless Networks with Reconfigurable Antennas

Yanjun Pan*, Ming Li*, Neng Fan*, and Yantian Hou†
*The University of Arizona, Tucson, AZ
†Boise State University, Boise, ID
Email: *{yanjunpan,lim,nfan}@email.arizona.edu, †yantianhou@boisestate.edu

***Abstract*—Reconfigurable antenna (RA) has emerged as a disruptive antenna technology with the potential of significantly improving the capacity of wireless links, by agilely reconfiguring its antenna states. Through jointly optimizing antenna state selection, routing and scheduling, it offers another dimension of opportunity to enhance end-to-end (E2E) throughput in multi-hop wireless networks (MWNs). However, the throughput limit of MWNs with RAs has not been well understood, due to challenges in theoretical modeling and computational intractability caused by a large number of states. In this work, we endeavor to systematically study this problem. We first propose a general antenna state-link conflict graph model to capture the intricate state-link association and corresponding interference relationship in the network. Based on this model, we formulate a max-flow based optimization framework to derive the throughput bound of a given MWN. As this problem is NP-hard, we explore column generation to solve it more efficiently, and propose a heuristic algorithm which can also accelerate the optimal solution. Simulation results show that our proposed algorithms can efficiently approach or compute the optimal throughput, and validate the advantage of antenna reconfigurability in MWNs.**

I. Introduction

Designing high performance Multi-hop Wireless Networks (MWNs) has remained challenging, despite past two decades' research [1], [2]. There are three main fundamental reasons: 1) Unreliable wireless links caused by multi-path fading or mobility; 2) The interference among wireless links due to the broadcast nature of wireless medium, especially in dense deployments; 3) The requirement for the network to adapt agilely to topology changes and traffic needs. Most existing solutions try to address these challenges from various layers (e.g.: error-correction coding/power control, multi-path/opportunistic routing [3], network coding [4], and etc.), however, they all do so by introducing extra redundancy/overhead or at a cost of other resources (e.g., energy). None of them can alter the fundamental characteristics of the physical wireless channel itself, which leads to limited performance gains.

In recent years, Reconfigurable Antenna (RA) [5] has emerged as a disruptive antenna technology which offers a promising alternative to solve the above challenges at the physical layer. RAs can change their own structures to achieve agile reconfigurability in radiation patterns, frequency, polarization, or combinations of them. For example, one type of RA can have thousands of different states and can be electronically switched within microseconds [5]. Compared with traditional antennas, RAs can perform multiple functions by dynamically changing its properties, which results in a significant reduction in size (one RA can replace multiple traditional antennas). Thus, RAs can be used as important additional degrees of freedom in a communication system resulting in significant additional gains. For example, it can enhance link capacity and reliability [6], achieve better interference alignment [7], and transmission scheduling in cellular networks [8].

This work was supported in part by ONR YIP award N00014-16-1-2650, and NSF grants CNS-1564477, CNS-1619728.

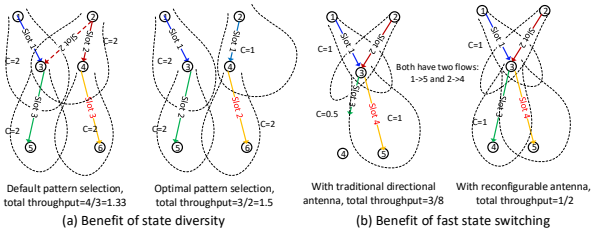

Fig. 1: Motivating examples: RA can enhance E2E throughput in MWNs due to its state diversity and fast reconfigurability

Yet, how to fully exploit the benefit of RAs in a MWN is still under-explored. We first present two simple motivating examples in Fig. 1. In Fig. 1 (a), a two-flow case shows the benefit of state diversity. In the left subfigure, node 2 uses the default state that maximizes the gain of link 2→4, but it also interferes with the 1→3 link. Thus nodes 1 and 2 have to transmit at separate time slots. In the right subfigure, optimal state selection is used such that node 2 adopts another state (e.g., a different pattern) which yields lower capacity for link 1→3, but now 1→3 and 2→4 can transmit simultaneously in slot 1, which yields a higher E2E throughput. In Fig. 1 (b), a two-flow case is shown to illustrate the benefit of fast state switching. Using traditional directional antennas (DAs) with a fixed beam, initially there is one flow (1→ 5) so the DA beam at node 3 is optimized to point toward node 5; but later when the 2→4 flow arrives, link 3→4's capacity is degraded by half due to fixed beam direction at node 3. While using RAs, node 3's transmitting state can be quickly adjusted such that 3→4 link's capacity remains the same, which again enhances total E2E throughput. Note that, the capacity gain of RAs comes at no cost of higher energy consumption, or alternatively, it can achieve higher energy-efficiency.

Though it is relatively easy to quantify the gains of RA for small-scale networks, it is very challenging for a general, large-scale multi-hop network. This is because: 1) The dynamic relationship between a wireless link and its antenna state. In existing models, one link uniquely corresponds to an antenna state. But with RAs, a link can be established in multiple states at different times. This necessitates new link layer models, which must be general enough to capture arbitrary antenna states; 2) The large number of antenna configurations available at each node and the exponential number of state combinations among all the nodes in the network; 3) The need to jointly consider the antenna configurations at each node, link scheduling and routing decisions for each flow in the network, which are interdependent. Considering all the above aspects, the optimization problems can easily be intractable.

In this paper, we make the first attempt to characterize the fundamental throughput limit of an arbitrary given MWNs equipped with RAs. To resolve the challenges in modeling, we employ the conflict graph methodology and propose a state-link conflict graph that captures the intricate state-link association and corresponding interference relationship in the network. We then establish a max-flow based optimization framework to find the throughput bound. Since directly solving it involves finding all the independent sets (ISs) of the state-link conflict graph, which is a well-known NP-hard problem, we exploit the column-generation approach to solve it without knowing the entire ISs in the state-link conflict graph in advance. Since the problem's complexity still depends on the conflict graph size, we propose a heuristic algorithm that prunes the original conflict graph to significantly reduce the input size before running column-generation. The independent set obtained by this algorithm can be fed as a good initial input into the optimal algorithm (with the original conflict graph), which can dramatically reduce the running time. In summary, our main contributions are three-fold:

1) We propose a novel state-link conflict graph for MWNs that captures the relationship between antenna state selection, link coverage, and interference. In addition, our model is general as it supports arbitrary types of antenna state (pattern, polarization or frequency).

2) Based on the new model, we develop a tractable max-flow based methodology to derive the throughput bounds of MWNs with RAs, by jointly optimizing antenna state selection, routing and scheduling. We use the column generation technique to efficiently solve this problem, and propose a conflict-graph pruning based heuristic algorithm to further accelerate the optimal solution. The heuristic itself can also be used as an approximation algorithm.

3) Extensive simulations based on a real RA's radiation patterns are carried out to validate the efficiency and effectiveness of our algorithms, in terms of approximation ratio and running time, and throughput gain compared with traditional methods. We show that the proposed optimal algorithm significantly outperforms the straightforward column-generation based approach, and also a previous approximation algorithm.

The remainder of the paper is organized as follows. Related works are reviewed in Sec. II. In Sec. III, we present the novel state-link conflict graph model for MWNs, based on which we formulate the column-generation based throughput optimization problem. The heuristic algorithm and the optimal algorithm are described in details in Sec. IV, followed by simulation results in Sec. V. Sec. VI concludes the paper.

II. Related Work

One of the major approaches to analyze the capacity in MWNs is to study their asymptotic capacity, which was initiated by Kumar and Gupta [1] and extended to mobile ad hoc networks by Grossglauser and Tse [2]. It was shown that the throughput per node decreases as N increases when using both protocol model and physical model. Later various antenna techniques have been applied to enhance the performance of MWNs [9], [10]. Li et al. [10] showed directional antennas (DAs) with random antenna patterns can lead to better scaling laws than omni-directional antennas (OAs).

Another category is to derive the concrete throughput bound for a given MWN topology. In [11], Jain et al. first proposed a conflict-graph based interference modeling approach to derive the max-flow throughput in a single source-destination pair MWN. Based on conflict graphs, numerous approaches have been proposed to compute the throughput bounds of MWNs. However, the link scheduling directly relates to ISs in the conflict graph, which makes it a NP-hard problem in general. Efficient approximation algorithms have been designed to schedule the links [12], [13]. However, the routing and scheduling are solved separately, which leads to an extra gap between approximation and optimum. On the other hand, concrete throughput bounds can be calculated from optimization techniques. In [14], Zhang et al. adopted column generation technique to jointly optimize routing and scheduling, but they minimized overall system activation time by solving its combinatorial formulation directly, which can be both time-consuming and memory-consuming for large-scale problems. Based on a similar framework, [15] proposed an ϵ-bounded approximation algorithm for minimum length scheduling problem in multi-hop multi-radio cellular networks. The NP-hard part of the problem (corresponding to the maximum weighted independent set, MWIS) was relaxed to its linear programming form, so as to find an IS by sequentially rounding up and fixing the linear solution. Though an error bound is defined in [15], the relaxation process destroyed the structure of column generation, which results in difficulties in convergence for large-scale problems. As we will show in Sec. V, the running time is unacceptable for our problem.

The MWNs in the above works are equipped with traditional omni-directional antennas (OAs). Authors in [16], [17] studied the concrete throughput bounds of MWNs with DAs/smart antennas. In [16], Huang et al. computed the throughput of a MWN with DAs based on a max-flow framework. However, the antenna pattern is predetermined and excluded from optimization variables. Ramanathan [18] analyzed the simulation-based throughput of MWNs using beamforming antennas without

TABLE I: Main Notations

V_n	Node set in the network
E_n	State-link set in the network
V	Vertex set in the conflict graph
E	Edge set in the conflict graph
L	Session set
$\mathcal{Q}/\mathcal{Q}'$	Set/subset of all the ISs in the conflict graph
$\mathcal{P}_i$	Candidate state set of node i
$\mathcal{T}_{i,u}/\mathcal{I}_{i,u}$	Transmission/interference set of node i under state u
$r(l)$	Total flow rate of session l
$s(l)/d(l)$	Source and destination of session l
$f_{i,j}^{u,v}(l)$	Flow rate of session l over link (i,j) under state (u,v)
λ_q	Time-share that IS $\mathcal{I}_q$ is scheduled
$c_{i,j}^{u,v}$	Capacity of link (i,j) under state (u,v)
$t_{i,j}^{u,v}(\mathcal{I}_q)$	Equals 1 if link (i,j) under state (u,v) is in IS, and is 0 otherwise $\mathcal{I}_q$
$x_{i,j}^{u,v}$	Vertex in the conflict graph that corresponds to link (i,j) under state (u,v)

mathematical formulation. Beamforming antennas are also exploited to enhance channel gain [19], but those works focus on protocol design without E2E throughput optimization. Recently RAs are employed to improve link capacity and reliability in MWNs. Yallmaz et al. [20] studied the sub-optimal throughput results of a single-hop cognitive heterogeneous network with pattern reconfigurable antennas. Hou et al. [21] first presented a throughput optimization framework of MWNs with RAs. However, their goal was to seek an optimal scheduling strategy under a given routing scheme, while the time was slotted and a finite number of slots were considered. In contrast, in this paper we aim at deriving a throughput bound independent from concrete scheduling schemes.

III. Modeling and Formulation

In this section, we first propose a novel *state-link conflict graph* model to characterize the interference relationship among the links in a MWN with RAs. Based on the new model, a throughput optimization framework with all ISs is developed. Then column generation technique is used to decompose this problem.

A. Antenna State-Link Conflict Graph Model

Conflict graphs have been widely adopted to compute the throughput bounds of MWNs in the past. The basic idea is to examine which "links" can be scheduled to transmit simultaneously. Traditionally, the graph is defined only based on links, however, with RAs, the interference relationship does not depend solely on link activation but also antenna states. Therefore, we propose a *state-link conflict graph* model to characterize the interference relationship among the links in a MWN with RAs.

For the antenna model, suppose each node i's antenna has a candidate state set as $\mathcal{P}_i$. Denote the transmitting gain of transmitter i's RA in the direction $\theta_{i,j}$ of link (i,j) as $G_{T_i}(u,\theta_{i,j})$, which depends on its transmitting antenna state $u \in \mathcal{P}_i$. Correspondingly, the receiving gain of a receiver j's RA is $G_{R_j}(v,\theta_{i,j})$ where v is the receiving antenna state. Then j's received power can be expressed as: $P_r(j) = P_t(i)L_{i,j}f(u,v)$, where $P_t(i)$ is i's transmission power, $L_{i,j}$ is the path loss of the physical channel between nodes i and j, and $f(u,v)$ is a function that specifies the impacts of RAs' states to the channel. For example, we can instantiate this function when the antenna is: 1) only pattern reconfigurable, $f(u,v) = G_{T_i}(u,\theta_{i,j}) \cdot G_{R_j}(v,\theta_{i,j})$; 2) only polarization reconfigurable, $f(u,v)$ is the polarization loss factor between i's transmitting antenna and j's receiving antenna. When both polarizations are linear, $f(u,v) = G_{T_i}G_{R_j}\cos^2\phi$, where ϕ is the angle between the two polarization directions; 3) only frequency reconfigurable, $f(u,v) = G_{T_i}G_{R_j}$ if u and v have the same frequency, otherwise $f(u,v) = 0$. It is straightforward to extend to any combinations of reconfigurable state types.

As an initial step to the new state-link conflict graph model, let's consider the protocol interference model [1], where a node j with state v is considered as within the transmission set $\mathcal{T}_{i,u}$ (or interference set $\mathcal{I}_{i,u}$) of node i under state u if $P_r(j) > P_T$ (or $P_r(j) > P_I$), where P_T and P_I is detection and interference threshold respectively. Note that, each element in transmission/interference set is a state-node pair instead of the node itself. Thus, two state-link pairs (i,j,u,v) and (i',j',u',v') interfere with each other if they cannot transmit simultaneously. Moreover, the combination of states-nodes are exponential, but the number of vertices in the state-link conflict graph is at most $|V_n|(log|V_n|)|\mathcal{P}_i||\mathcal{P}_j|$ because each node needs to have $\Theta(log|V_n|)$ neighbors on average to achieve asymptotic connectivity [22]. Hence based on the state-link conflict graph, the sets of concurrently transmitting state-link pairs can be found.

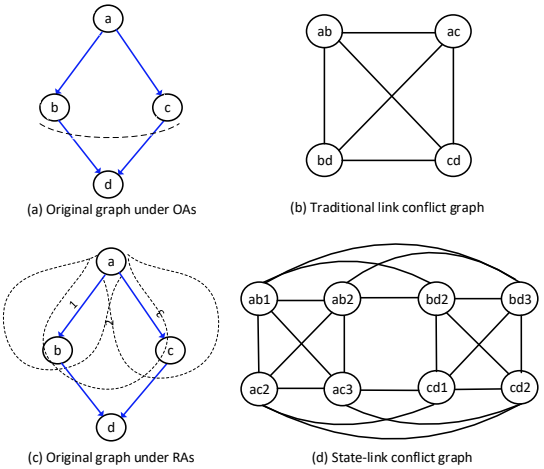

Fig. 2: Conflict Graph

To illustrate this idea, we use a simple example shown in Fig. 2. To simplify, we consider transmitting antenna pattern-reconfigurability only, and assume that all nodes work in half-duplex mode. The original four-node network graph under OAs is shown in Fig. 2 (a). Fig. 2 (b) shows the traditional link-based conflict graph using OAs, where the ISs are $\{ab\},\{bd\},\{ac\},\{cd\}$ (only one link can transmit at a time). With RAs, the original network graph is shown in Fig. 2 (c), where each node's RA has the same set of three transmitting states indexed by $\{1,2,3\}$. Its corresponding conflict graph's vertices are state-link pairs (Fig. 2 (d)). It can be seen that the new ISs are: $\{ab1,cd1\}$, $\{ab1,cd2\}$, $\{ab2,cd1\}$, $\{ab2,cd2\}$,

$\{ac2, bd2\}$, $\{ac2, bd3\}$, $\{ac3, bd2\}$, $\{ac3, bd3\}$, where two-link simultaneous transmissions become possible.

In general, for a MWN which can be modeled as a directed graph $G(V_n, E_n)$, where $(i,j) \in E_n$ when $(j,v) \in \mathcal{T}_{i,u}$, we can establish its corresponding state-link conflict graph as $G_c(V, E)$, where the vertex set V is the set of state-link pairs in G. Namely that a vertex $x_{i,j}^{u,v}$ in the state-link conflict graph corresponds to a state-link pair defined as (i, j, u, v), where $u \in \mathcal{P}_i, (i,j) \in E_n$. In the conflict graph G_c, there is an edge between any two vertices if they are in conflict with each other. Thus, two vertices $x_{i,j}^{u,v}, x_{i',j'}^{u',v'}$ in the state-link conflict graph are adjacent if: (1) A node selects more than one state at a certain time, i.e. $(x_{i,j}^{u,v}, x_{i,j'}^{u',v'}) \in E, \forall u \neq u'$; (2) A node transmits to/receives from multiple nodes at a certain time, i.e. $(x_{i,j}^{u,v}, x_{i,j'}^{u',v'}) \in E, \forall j \neq j'$ or $(x_{i,j}^{u,v}, x_{i',j}^{u',v'}) \in E, \forall i \neq i'$; (3) A node works in a full duplex mode, i.e. $(x_{i,j}^{u,v}, x_{j',i}^{v',u'}) \in E$; (4) The receiver of one state-link pair is interfered by another state-link pair's transmitter, i.e. $(x_{i,j}^{u,v}, x_{i',j'}^{u',v'}) \in E$, $\forall (j', v') \in \mathcal{I}_{i,u}$ or $(j,v) \in \mathcal{I}_{i',u'}$.

B. Maximum Flow Based Optimization Framework

1) Routing Constraints: Denote the flow rate of session l over state-link pair (i,j,u,v) as $f_{i,j}^{u,v}(l)$, and the aggregate flow rate of session l as $r(l)$. Then we have:

$$\sum_{j:(s_l,j)\in E_n} \sum_{u\in\mathcal{P}_{s_l}} \sum_{v\in\mathcal{P}_j} f_{s_l,j}^{u,v}(l) - \sum_{i:(i,s_l)\in E_n} \sum_{u\in\mathcal{P}_i} \sum_{v\in\mathcal{P}_{s_l}} f_{i,s_l}^{u,v}(l) = r(l),\ \forall l \in L \quad (1)$$

$$\sum_{i:(i,d_l)\in E_n} \sum_{u\in\mathcal{P}_i} \sum_{v\in\mathcal{P}_{d_l}} f_{i,d_l}^{u,v}(l) - \sum_{j:(d_l,j)\in E_n} \sum_{u\in\mathcal{P}_{d_l}} \sum_{v\in\mathcal{P}_j} f_{d_l,j}^{u,v}(l) = r(l),\ \forall l \in L \quad (2)$$

$$\sum_{j:(i,j)\in E_n} \sum_{u\in\mathcal{P}_i} \sum_{v\in\mathcal{P}_j} f_{i,j}^{u,v}(l) = \sum_{j:(j,i)\in E_n} \sum_{u\in\mathcal{P}_j} \sum_{v\in\mathcal{P}_i} f_{j,i}^{u,v}(l), \quad \forall i \in V_n \backslash \{s_l, d_l\},\ \forall l \in L \quad (3)$$

where $s(l)$ and $d(l)$ represent the source and destination of session l. Constraints (1) and (2) indicate that the aggregate flow rate of session l is flows generated from the source intended for the destination. And constraint (3) implies that for any intermediate nodes, overall incoming flows must balance with overall outgoing flows.

2) Scheduling Constraints: Suppose that we can list all the ISs as set $\mathcal{Q}$ for the conflict graph. To avoid interference, there can be only one activated IS at any time. Denote the time-share that IS $\mathcal{I}_q$ is scheduled as λ_q. Then:

$$\sum_{l\in L} f_{i,j}^{u,v}(l) \leq \sum_{q=1}^{\mathcal{Q}} \lambda_q \cdot [c_{i,j}^{u,v} \cdot t_{i,j}^{u,v}(\mathcal{I}_q)],\ \forall (i,j) \in E_n, \quad \forall u \in \mathcal{P}_i,\ \forall v \in \mathcal{P}_j \quad (4)$$

$$\sum_{q=1}^{\mathcal{Q}} \lambda_q \leq 1 \quad (5)$$

where $c_{i,j}^{u,v}$ is the capacity of link (i,j) under state (u,v). And constraint (4) is the capacity constraint for every state-link pair.

3) Primal Problem: For a MWN with RAs, based on all the ISs in its corresponding state-link conflict graph, we can formulate its throughput optimization problem via joint antenna state selection, routing and scheduling as:

$$\textbf{PP:} \quad \max \sum_{l\in L} r(l)$$
$$\text{s.t.} \quad \text{Equations } (1) - (5)$$
$$f_{i,j}^{u,v}(l) \geq 0,\ \forall (i,j) \in E_n,\ \forall u \in \mathcal{P}_i,\ \forall v \in \mathcal{P}_j,\ \forall l \in L$$
$$\lambda_q \geq 0,\ \forall q \in \mathcal{Q}$$

All variables and parameters are shown in Table I.

Generally, finding all the ISs in a graph is NP-hard, which makes it is difficult to obtain set $\mathcal{Q}$ and solve problem PP directly. Therefore, we adopt the column generation method to add a column (which is also a variable that corresponds to an IS in (4)) when needed.

4) Impact of Antenna State Switching Delay: In the above formulation, we omit the antenna switching delay due to the fast reconfigurability of RAs. Indeed, our model is applicable for any types of antennas. Considering an antenna with slow switching (e.g. steered beam antennas), no matter how large the delay is, it still costs a finite time. Since our model considers time-sharing, any given time-share can be realized by finding a feasible time period length for each IS that includes the switching delay.

C. Decomposition: Column Generation Based Approach

In large-scale linear programming problems, most of the variables are non-basic and assume to be zero in the optimal solution, hence only a subset of variables need to be considered when solving the problem. Column generation leverages this idea to generate only the variables which have the potential to improve the objective function [23]. In our case, by starting with $\mathcal{Q}' \subseteq \mathcal{Q}$, constraints (4) and (5) are restricted to:

$$\sum_{l\in L} f_{i,j}^{u,v}(l) \leq \sum_{q=1}^{\mathcal{Q}'} \lambda_q \cdot (c_{i,j}^{u,v} \cdot t_{i,j}^{u,v}(\mathcal{I}_q)),\ \forall (i,j) \in E_n, \quad \forall u \in \mathcal{P}_i,\ \forall v \in \mathcal{P}_j \quad (6)$$

$$\sum_{q=1}^{\mathcal{Q}'} \lambda_q \leq 1 \quad (7)$$

Then, we get the following restricted master problem (RMP):

$$\textbf{RMP:} \quad \max \sum_{l\in L} r(l)$$
$$\text{s.t.} \quad \text{Equations } (1) - (3) \text{ and } (6) - (7)$$

Note that RMP is a linear programming problem, so we can solve it optimally in polynomial time and get optimal solutions (including optimal dual solutions). Denote the dual solutions of

constraints (6) and (7) as $z_{i,j}^{u,v}$ and γ respectively, the occurring subproblem (SP) can be formulated as:

$$\textbf{SP:} \quad \max \ \delta = \sum_{(i,j)\in E} \sum_{u\in\mathcal{P}_i} \sum_{v\in\mathcal{P}_j} z_{i,j}^{u,v} \cdot c_{i,j}^{u,v} \cdot t_{i,j}^{u,v}(\mathcal{I}_q) - \gamma \tag{8}$$

$$\text{s.t.} \quad x_{i,j}^{u,v} + x_{i',j'}^{u',v'} \leq 1, \ \forall (x_{i,j}^{u,v}, x_{i',j'}^{u',v'}) \in E \tag{9}$$

$$x_{i,j}^{u,v} \in \{0,1\}, \ \forall x_{i,j}^{u,v} \in V$$

where $x_{i,j}^{u,v}$ is a binary variable defined by: if state-link pair (i,j,u,v) is in the IS $\mathcal{I}_q$, then $x_{i,j}^{u,v} = 1$; otherwise, $x_{i,j}^{u,v} = 0$. Thus, for two adjacent vertices $x_{i,j}^{u,v}$ and $x_{i',j'}^{u',v'}$, at most one of them can appear in the same IS, which is constraint (9). For SP, note that: 1) SP is essentially a MWIS problem; 2) $t_{i,j}^{u,v}(\mathcal{I}_q)$ is not a binary indicator in SP anymore. Alternatively, it becomes the q^{th} IS which consists of variables $x_{i,j}^{u,v}$, that is $t_{i,j}^{u,v}(\mathcal{I}_q) = \{x_{i,j}^{u,v} : x_{i,j}^{u,v} \in \{0,1\}, \ \forall x_{i,j}^{u,v} \in V\}$.

For column generation, in each iteration we solve RMP first, and substitute its dual solutions into the objective of SP. Then SP is solved and its optimal objective solution δ^* is checked. If $\delta^* \leq 0$, then there is no solution that can further improve the objective. Hence current solutions for RMP also optimally solve PP, and we terminate the iterative process. Otherwise, the optimal IS found in SP is added to RMP as a new column and we re-optimize RMP and SP repeatedly. In the following, we improve this approach by proposing a heuristic algorithm first, based on which an accelerated optimal algorithm is also presented.

IV. Heuristic and Optimal Algorithms

As mentioned before, SP is a MWIS problem indeed, which is a famous NP-hard problem. Typically, for a real-world RA which has a large number of antenna states, the state-link conflict graph can be extremely large that results in intolerable running time. Though some efficient algorithms for MWIS problems have been proposed, we cannot use them directly to SP because they would break the structure of column generation. Specifically, iteration terminates when $\delta^* \leq 0$, whereas the solution obtained from any approximation algorithm ($\underline{\delta}$) is a lower bound of δ^*. Even though $\underline{\delta} \leq 0$, $\delta^* > 0$ could still be the case. Also, since our goal is to find throughput bounds via jointly optimizing antenna pattern selection, routing and scheduling, it is difficult to develop an approximation algorithm without any prior knowledge of the optimal strategy. Here, we propose a conflict-graph pruning based heuristic algorithm (CPH), which can either be a standalone algorithm or also be used to accelerate the optimal solution.

A. Conflict-Graph Pruning Based Heuristic Algorithm

The basic idea is to prune the original conflict graph so as to reduce the size of input to the column-generation based solution. The pruning algorithm consists of two steps.

1) Finding Link-disjoint Paths: Considering that only a portion of state-link pairs is activated in optimal solutions, ideally, we only need to keep the activated state-link pairs and eliminate the unused ones. From our preliminary simulation results, we observe that most of the activated state-link pairs are link-disjoint. Thus, we could find link-disjoint paths using the existing max-flow algorithm for disjoint paths problems. Specifically, to find link-disjoint paths for each session, change the capacity of each link into one and solve the corresponding max-flow problem. This simple method works because the capacity of each link is reduced to one, a link cannot be used again in each session. Then by merging all the disjoint paths and extracting the corresponding state-link pairs, we can obtain the preliminary improved conflict graph as $G_c' = (V', E')$.

Algorithm 1 CPH Algorithm

Input: Initial independent set $\mathcal{Q}'$, the value for k.
Output: $\underline{r(l)}, \underline{f_{i,j}^{u,v}(l)}, \underline{\lambda_q}$.

```
for each l ∈ L do
    Run any max-flow algorithm to obtain the link-disjoint paths;
end for
Aggregate all the link-disjoint paths and obtain G_c' = (V', E');
for each x_{i,j}^{u,v} ∈ V' do
    (c_{i,j}^{u,v})' = c_{i,j}^{u,v} / N(x_{i,j}^{u,v});
end for
for each (i,j) ∈ G_c' do
    Sort (c_{i,j}^{u,v})' with non-increasing order, and obtain the set of
    top k (c_{i,j}^{u,v})' as C_{i,j};
end for
Obtain G_c'' = (V'', E''), where V'' = {x_{i,j}^{u,v} | (c_{i,j}^{u,v})' ∈
    C_{i,j}, ∀(i,j) ∈ G_c'};
while δ* > 0 do
    Solve RMP based on G_c'' optimally, obtain its optimal solutions
    r(l), f_{i,j}^{u,v}(l), λ_q and dual solutions z_{i,j}^{u,v}, γ;
    Solve SP optimally, obtain δ* and I_q = {x_{i,j}^{u,v} | ∀x_{i,j}^{u,v} ∈ V''};
    Update Q' = Q' ∪ I_q;
end while
```

2) Selecting Top-k Antenna States: Note that G_c' only cuts some links while the number of antenna states at each node unchanged, the size of G_c' can still be large when there are many antenna states. Hence we use a top k method to further improve G_c'. Notice that there are two main aspects that an antenna state can have impact on: 1) link capacity: under the same transmission power, the antenna state with higher gain in the given direction will provide higher capacity; 2) potential interference: for the similar shape of radiation pattern, the antenna state with higher gain might interfere with more links. To balance the positive contribution and negative impact of each antenna state to the network flow, we update the capacity of state-link pair (i,j,u,v) by: $(c_{i,j}^{u,v})' = c_{i,j}^{u,v} / N(x_{i,j}^{u,v})$, where $N(x_{i,j}^{u,v})$ is the number of neighbors of vertex $x_{i,j}^{u,v}$ in G_c' which we regard as a rough estimation of the potential interference that vertex $x_{i,j}^{u,v}$ can cause. Then we sort $(c_{i,j}^{u,v})'$ with non-increasing order for each link (i,j), and only select states of the top k $(c_{i,j}^{u,v})'$ as available states for link (i,j). In this way, the number of states for each link (i,j) is k at most and we define the secondary improved conflict graph obtained from

top k method as $G_c'' = (V'', E'')$. The detailed CPH algorithm is described in Alg. 1.

B. Optimal Algorithm

A straightforward method to solve our problem is to easily form set $\mathcal{Q}'$ by the set of independent sets which each of them only contains one vertex in the conflict graph. However, it is time-consuming for RMP to converge due to degeneracy [24], especially for large-scale problems (a linear programming is degenerate if it has at least one basic feasible solution where a basic variable is equal to 0). Hence we propose an optimal algorithm which uses CPH algorithm to accelerate the optimal solution. The algorithm is called RedOpt since it can reach optimum with a largely reduced running time compared with the straightforward method. The detailed RedOpt is described in Alg. 2, and the basic idea is that instead of starting with set $\mathcal{Q}'$, we add the set of independent sets obtained from Alg. 1 ($\mathcal{Q}''$) as initial independent sets. Thus, by starting with set $\mathcal{Q}''$, RMP starts with a much tighter solution found by Alg. 1 than the straightforward method. Besides, set $\mathcal{Q}''$ performs better than ISs found by any approximation algorithm of MWIS because the latter one decouples ISs from the overall objective and find uncorrelated ISs to the need of throughput maximization. Note that RedOpt is an optimal algorithm since we use the original conflict graph as the input, and the optimality is guaranteed by column generation procedure.

Algorithm 2 RedOpt Algorithm

Input: Initial independent set $\mathcal{Q}'$, the value for k.
Output: $r^*(l), f_{i,j}^{u,v*}(l), \lambda_q^*$.

```
Solve RMP and SP with Algorithm 1 and obtain Q'';
Add Q'' as Q' to constraint (6)-(7);
while δ* > 0 do
    Solve RMP based on original conflict graph G_c optimally;
    Solve SP optimally, obtain δ* and I_q = {x_{i,j}^{u,v} | ∀x_{i,j}^{u,v} ∈ V};
    Update Q' = Q' ∪ I_q;
end while
```

C. Computational Complexity Analysis

The first and second step of Alg. 1 can be implemented in polynomial time since only classical algorithms such as maximum-flow and sorting are involved. The most complex components for Alg. 1. and Alg. 2 are both the large-scale combinatorial part. Hence their computational complexity is dominated by problem SP. Considering that each node needs to have $\Theta \log n$ neighbors on average to achieve asymptotic connectivity, Alg.1 and Alg 2. will take $O(2^{|V''|}) = O(2^{|V_n'|(log|V_n'|)k^2})$ and $O(2^{|V_n|(log|V_n|)|\mathcal{P}_i||\mathcal{P}_j|})$ time respectively in the worst case, where V_n' is the set of nodes on link-disjoint paths. Note that, in the pruned conflict graph, $|V_n'| < |V_n|$ and k is a constant that makes $k^2 << |\mathcal{P}_i||\mathcal{P}_j|$. Therefore, Alg.1 is efficient in practice. Furthermore, though the optimal algorithm Alg. 2 has the same worst case complexity as the straightforward method mentioned in Sec. IV-B, it performs better by starting from a good initial independent set found by Alg. 1. In this way, the degeneracy is relieved and considerable running time can be saved consequently.

V. Simulation Results

In this section, we implement extensive simulations based on a real RA's radiation patterns to evaluate proposed algorithms. Although our model is general, we only evaluated it using a pattern-reconfigurable antenna due to resource limitations. All the formulations and algorithms are implemented in MATLAB using CPLEX 12.7.1, and all computations are performed on a Windows machine with Intel (R) Core(TM) CPU 3.6GHz processors and 32GB RAM.

A. Simulation Setup

We place 20 nodes randomly distributed in a 60×60 square unless otherwise stated. The transmission and interference threshold is $-55dBm$ and $-65dBm$ respectively. We use a free-space propagation model where the path loss factor is 4 and set the transmission power and noise level to be $0dBm$ and $-95dBm$ respectively. To simplify, we consider transmitting antenna state reconfigurability only. Thus, we omit the notation of receiver's antenna state for all the variables and state-link pairs, i.e. $f_{i,j}^{u,v} \rightarrow f_{i,j}^{u}$ and etc..

The 3D view of the RA we use is shown in Fig. 3 (a). The RA is designed to steer its beams into nine directions ($\theta \in \{-30°, 0°, 30°\}, \phi \in \{0°, 45°, 90°, 135°\}$), by reconfiguring the geometry of the parasitic pixel surface which consists of 3×3 square-shaped metallic pixels that are connected by 12 p-i-n diode switches [25]. Each switch has ON and OFF status, which brings 4096 possible modes of operation to the RA. In practice, there are 253 antenna states with known antenna gains that match our reflection coefficient constraints. We select 100 of them with appropriate gains (not too big or too small) and depict their radiation patterns in Fig. 3 (b).

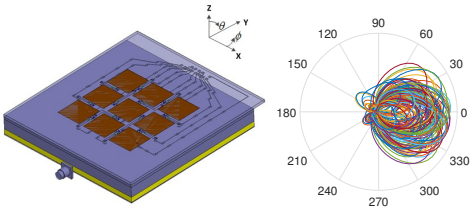

(a) (b)

Fig. 3: Subfigure (a) shows 3D view of the RA. (b) shows radiation patterns of the 100 states in the plane of $\phi = 90°$.

B. Case Study

In this part, we use an example to show the benefits brought from RAs. We generate two sessions that are 4→18 and 15→2 in the network. To start, we set $k = 10$ for Alg. 1 and list the size of conflict graph and obtained throughput in Table II. We can see that: 1) The CPH algorithm saves numerous memory: the number of vertices and edges in G_c increases dramatically when the number of antenna states increases; in contrast, the size of G_c'' increases much slower. 2) When the number of antenna states is 80-100, the RedOpt algorithm cannot solve the problem due to the memory overflow, however, the CPH algorithm still works and gives out a lower bound of the network throughput; 3) When looking into the details of

optimal routing and scheduling strategies obtained, we can see the benefits brought from state diversity and swift pattern switching. To illustrate, we depict the optimal strategy obtained from RedOpt when the number of antenna states is 20 in Fig. 4. Here we depict the state-link pairs appeared in the same IS with the same color and we can see that for link (15,3), node 15 utilizes state 2 and 6 in different time-shares; 4) The throughput improvement increases slowly with the number of antenna states because of the antenna itself. As shown in Fig. 3 (b), many states are similar. In fact the slow improvement exhibits a *diminishing return* phenomena: with more antenna states, the less the gain. Up to certain number of states, the network already has enough spatial coverage, and sometimes the optimal states are already there, so that not much additional benefits can offer for additional ones look similar in shape; 5) The gap of the throughput obtained from CPH and RedOpt is small, we hypothesise that CPH algorithm might be able to approximate to the optimal solution with high accuracy.

TABLE II: Size of conflict graph G_c and G_c'', as well as the total throughput of the network, where $|\mathcal{P}_i|$ is the number of antenna states

	RedOpt			CPH ($k = 10$)		
$\lvert\mathcal{P}_i\rvert$	$\lvert V\rvert$	$\lvert E\rvert$	Throughput	$\lvert V''\rvert$	$\lvert E''\rvert$	Throughput
20	2667	2945263	9.403610	344	48668	9.263092
30	4015	6759328	9.415474	391	61677	9.281410
40	5335	11937936	11.147821	402	61780	10.873429
50	6656	1866624	12.246594	409	62908	11.688579
60	7990	26947751	12.254678	414	64776	11.706540
70	9281	36242999	12.289423	421	65890	11.731324
80	10567	46518022	—	422	63980	11.735903
90	11900	59150782	—	424	64168	11.734532
100	13225	72418827	—	424	62628	11.769862

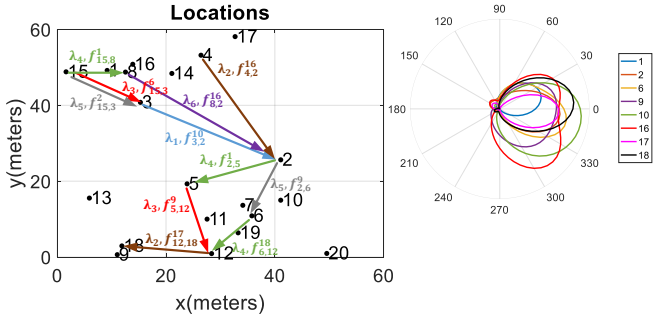

Fig. 4: When there are 20 antenna states, the optimal routing and scheduling strategy as well as radiation patterns of activated antenna states for the case study

C. Performance of Proposed Algorithms

To verify our hypothesis, here we use more numerical results to evaluate the performance of CPH algorithm. Here we set the parameter k in CPH algorithm as $k = 10$.

1) Impact of Number of Sessions: First we consider the impacts of the number of sessions. The source and destination of each session are randomly generated and the number of antenna states are fixed as 40. We increase the number of sessions from 2 to 6 and simulate 10 scenarios for each session amount. The results are shown in Fig. 5, we can see that: 1) CPH algorithm can effectively approximate to the optimal solution with high accuracy; 2) In general, the running time increases with the number of sessions for both algorithms since the number of variables and constraints increases proportionally to the number of sessions; 3) Note that when the number of sessions is 6, the RedOpt is less than that when there are 5 sessions in the network, which seems to be counterintuitive. To understand this phenomenon, we need to clarity that the time to solve each subproblem does increase with the size of the conflict graph. However, the total running time for reaching optimum also relies on the number of iterations, which depends on the degeneracy situation of the problem. Since the degeneracy is not proportional to the size of conflict graph, the running time for RedOpt fluctuates.

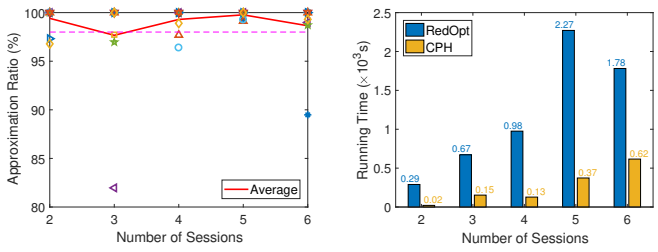

(a) (b)

Fig. 5: Impact of Number of Sessions: fix the number of antenna states to 40 and randomly generate sessions

2) Impact of Number of Antenna States: Since the randomly generated sessions always confronted with fairness issues, we fix the number of sessions to 2 and select 10 scenarios that both sessions can be activated simultaneously to guarantee fairness. Note that, under these kinds of settings, CPH algorithm would perform worse than the scenarios under randomly generated sessions, since for random cases only one of the sessions would be activated via relatively less hops. Especially, the antenna state that connects the source and destination with maximum link capacity is usually selected as the optimal solution. Under these scenarios, CPH algorithm would find the optimal solution with high probability due to followings: First, since the routing is $s \rightarrow t$ itself, the link is definitely reserved. Second, the capacity would dominate the capacity updating process, so that the antenna state provides larger link capacity is very likely to be reserved. The results are shown in Fig. 6 and we can observe that: 1) Similarly, CPH algorithm is capable of effectively approximating to the optimal solution; 2) Compared with previous results, we can see that the approximation ability of CPH performs better in random session cases, which implies that it also has a good performance in general.

In conclusion, the CPH algorithm can either provide a good initial input to RMP to accelerate the convergence speed, or it can be used as a standalone algorithm itself, when the exact optimal solution is not strictly required and the running time is intolerable due to large instance size.

3) Antenna State Selection Benefits: To validate the superiority of jointly optimizing antenna state selection, we

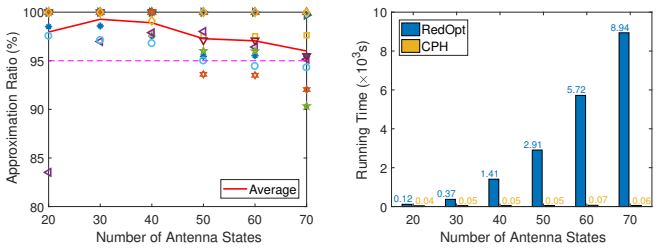

(a) (b)

Fig. 6: Impact of Number of Antenna States: fix the number of sessions to 2 and 10 selected sessions

simulate the joint routing and scheduling optimization only. We predetermine the antenna state to the pattern resulting in highest signal power [16], which is equivalent to choose the antenna pattern that results in maximum link capacity. Hence $c_{i,j} = \arg\max_{u \in \mathcal{P}_i} \{c^u_{i,j}\}$. By using the same setting as Sec. V-C2, we show the average approximation ratio with/without antenna state selection (ASS) in 7 (a). Obviously, the average approximation ratio of the network throughput reduces about 20% without optimal antenna state selection.

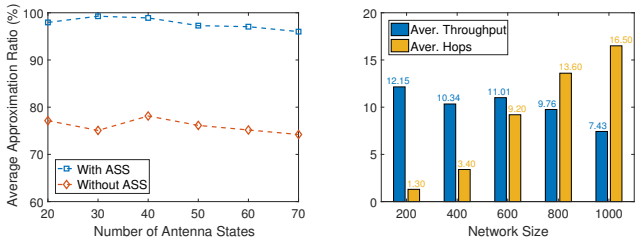

(a) (b)

Fig. 7: Subfigure (a) shows the average approximation ratio with/without antenna state selection. (b) shows the average throughput and number of hops under different network size

4) Scalability: To explore the performance of proposed algorithms in large-scale networks, we fix the density of the network to $\frac{10}{200\times200}$ nodes per unit area. And increase the side length of the square from 200 to 1000. Under each network size, we randomly generate 10 scenarios. To guarantee the connectivity of the network, we increase the transmission power from $0dBm$ to $15dBm$. The number of sessions and antenna states is 2 and 20 respectively. The results are shown in Fig. 7 (b), and we can observe that: 1) By increasing the network size, more hops are activated on a session. The reason is straightforward as a larger network has a larger distance between source and destination on average, more nodes and links are needed on a path; 2) Though the average throughput has a tiny fluctuation when the network is 600×600 due to randomness on sessions. In general, with the increase of average hop count, the average throughput decreases as expected. This is because more hops bring more competitions within the network due to interference, which reduces the flow rate on each session. However, the decrease is graceful, which shows the benefit of directivity and coverage of RA's patterns.

D. Comparison

In this part, we compare the performance of RedOpt with the straightforward method and the ϵ-Bounded approximation algorithm proposed in [15] (which is the most similar work to us). To simplify, we name the straightforward method mentioned in Sec. IV-B as "original column generation based optimal solution" (OCGOpt). We select 4 scenarios from Sec. V-C1, where the number of sessions and antenna states are fixed to 2 and 40 respectively. Especially, the selected first two scenarios are beneficial to OCGOpt and the ϵ-bounded algorithm because the optimal scheduling is a state-link pair consisted of source-destination that makes optimization process less time-consuming. On the other hand, to show the effectiveness of concurrent transmissions, the last two scenarios are selected from scenarios that both sessions are activated. Moreover, the threshold for the running time of OCGOpt and the ϵ-bounded algorithm is set to be 12 hours to avoid endless loops.

1) RedOpt v.s. OCGOpt: Both methods are implemented on the original state-link conflict graph whereas RedOpt starts with the independent set found by CPH algorithm while OCGOpt takes each vertex in the conflict graph as an independent set. The results show that in all the scenarios, for OCGOpt, the iteration terminates due to time limit instead of convergence criterion, meaning that the running time for OCGOpt exceeds 12 hours, while RedOpt takes much less time to converge to the optimal solution (as shown in Fig. 5 (b)). The achieved throughput is shown in Fig. 8 (a). We also plot the initial throughput for OCGOpt (that is, only solve RMP once by adding set $\mathcal{Q}'$ described in IV-B) to reflect the improvement. From Fig. 8 (a), we can see that for all the scenarios the throughput obtained from OCGOpt after running 12 hours is equal to the corresponding initial solution, which implies the severe degeneracy of the problem. Besides, the degeneracy is also the main reason that RedOpt outperforms OCGOpt. By starting with a good independent set, many points that lead to degeneracy are avoided.

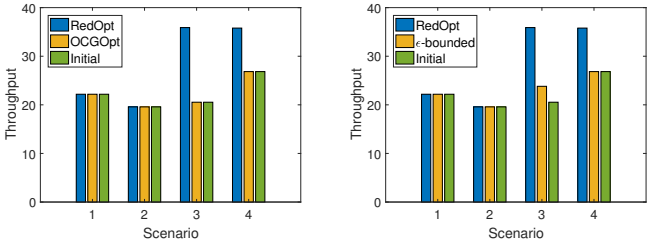

(a) (b)

Fig. 8: Throughput obtained from RedOpt and OCGOpt/ϵ-bounded algorithm (within a time limit of 12 hours)

2) RedOpt v.s. ϵ-Bounded Approximation Algorithm: Here we compare the performance of the ϵ-bounded algorithm with our RedOpt algorithm. To provide the algorithm in [15] with some extra advantages, we set $\epsilon = 5\%$ and adapt the same

approximation procedure (mentioned in Sec. II) to our problem. From the results in Fig. 8 (b) we can see that the ϵ-bounded algorithm has similar results with OCGOpt: 1) The iteration terminates due to time limit instead of convergence for all the scenarios; 2) The ϵ-bounded algorithm provides scenario 3 with some throughput improvements, but its overall performance is similar to that of OCGOpt; 3) For large-scale inputs to our problem, the ϵ-bounded algorithm has limited gains comparing with the RedOpt algorithm even though it has been executed more than 12 hours. The worse performance is mainly due to the linear relaxation and sequential fixing operations for the subproblem in [15]. Specifically, the half-integrality property [26] of the linear relaxation of MWIS problem restricts each of its linear solution to $\{0, \frac{1}{2}, 1\}$. Thus, different fixing order could have a remarkable impact on finding a satisfiable IS. Moreover, even though a satisfiable IS is found for the current iteration, due to the severe degeneracy in column generation technique, a large number of iterations are required to reach global optimum for a large-scale problem. Note that, the ϵ-bounded algorithm in [15] also has the same exponential complexity as RedOpt in the worst case.

VI. Conclusions

In this work, we studied the throughput bounds of MWNs with RAs. We proposed a novel and general state-link conflict graph model which captures the dynamic state-link relations. Based on our new model, a maximum-flow based optimization framework is formulated to derive the throughput limits of MWNs. Column generation is employed to efficiently solve the problem and an optimal algorithm that utilizes our novel heuristic algorithm to accelerate the optimal solution is also proposed. Extensive simulations are carried out to validate the efficiency and effectiveness of our algorithms. In the future, we will extend our model to handle the fairness issues in the network and consider practical aspects such as unreliable links/channels. Also, we plan to design efficient approximation algorithms and distributed algorithms that approach the performance limit.

References

[1] P. Gupta and P. R. Kumar, "The capacity of wireless networks," *Information Theory, IEEE Transactions on*, vol. 46, no. 2, pp. 388–404, 2000.

[2] M. Grossglauser and D. Tse, "Mobility increases the capacity of ad-hoc wireless networks," in *INFOCOM 2001. Twentieth Annual Joint Conference of the IEEE Computer and Communications Societies. Proceedings. IEEE*, vol. 3. IEEE, 2001, pp. 1360–1369.

[3] D. Ganesan, R. Govindan, S. Shenker, and D. Estrin, "Highly-resilient, energy-efficient multipath routing in wireless sensor networks," *ACM SIGMOBILE Mobile Computing and Communications Review*, vol. 5, no. 4, pp. 11–25, 2001.

[4] S. Katti, H. Rahul, W. Hu, D. Katabi, M. Médard, and J. Crowcroft, "Xors in the air: practical wireless network coding," in *ACM SIGCOMM Computer Communication Review*, vol. 36, no. 4. ACM, 2006, pp. 243–254.

[5] D. Rodrigo, B. A. Cetiner, and L. Jofre, "Frequency, radiation pattern and polarization reconfigurable antenna using a parasitic pixel layer," *Antennas and Propagation, IEEE Transactions on*, vol. 62, no. 6, pp. 3422–3427, 2014.

[6] A. Grau, H. Jafarkhani, and F. De Flaviis, "A reconfigurable multiple-input multiple-output communication system," *Wireless Communications, IEEE Transactions on*, vol. 7, no. 5, pp. 1719–1733, May 2008.

[7] T. Gou, C. Wang, and S. Jafar, "Aiming perfectly in the dark-blind interference alignment through staggered antenna switching," *Signal Processing, IEEE Transactions on*, vol. 59, no. 6, pp. 2734–2744, June 2011.

[8] E. Anderson, C. Phillips, D. Sicker, and D. Grunwald, "Optimization decomposition for scheduling and system configuration in wireless networks," *IEEE/ACM Trans. Netw.*, vol. 22, no. 1, pp. 271–284, Feb. 2014.

[9] S. Yi, Y. Pei, and S. Kalyanaraman, "On the capacity improvement of ad hoc wireless networks using directional antennas," in *Proceedings of the 4th ACM international symposium on Mobile ad hoc networking & computing*. ACM, 2003, pp. 108–116.

[10] P. Li, C. Zhang, and Y. Fang, "The capacity of wireless ad hoc networks using directional antennas," *IEEE Transactions on Mobile Computing*, vol. 10, no. 10, pp. 1374–1387, 2011.

[11] K. Jain, J. Padhye, V. N. Padmanabhan, and L. Qiu, "Impact of interference on multi-hop wireless network performance," in *Proceedings of the 9th Annual International Conference on Mobile Computing and Networking*, ser. MobiCom '03. New York, NY, USA: ACM, 2003, pp. 66–80.

[12] M. Kodialam and T. Nandagopal, "Characterizing achievable rates in multi-hop wireless networks: the joint routing and scheduling problem," in *Proceedings of the 9th annual international conference on Mobile computing and networking*. ACM, 2003, pp. 42–54.

[13] C.-Y. Hong and A.-C. Pang, "3-approximation algorithm for joint routing and link scheduling in wireless relay networks," *IEEE Transactions on Wireless Communications*, vol. 8, no. 2, pp. 856–861, 2009.

[14] J. Zhang, H. Wu, Q. Zhang, and B. Li, "Joint routing and scheduling in multi-radio multi-channel multi-hop wireless networks," in *Broadband Networks, 2005. BroadNets 2005. 2nd International Conference on*. IEEE, 2005, pp. 631–640.

[15] M. Li, S. Salinas, P. Li, X. Huang, Y. Fang, and S. Glisic, "Optimal scheduling for multi-radio multi-channel multi-hop cognitive cellular networks," *IEEE Transactions on Mobile Computing*, vol. 14, no. 1, pp. 139–154, 2015.

[16] X. Huang, J. Wang, and Y. Fang, "Achieving maximum flow in interference-aware wireless sensor networks with smart antennas," *Ad Hoc Networks*, vol. 5, no. 6, pp. 885–896, 2007.

[17] C. Peraki and S. D. Servetto, "On the maximum stable throughput problem in random networks with directional antennas," in *Proceedings of the 4th ACM international symposium on Mobile ad hoc networking & computing*. ACM, 2003, pp. 76–87.

[18] R. Ramanathan, "On the performance of ad hoc networks with beamforming antennas," in *Proceedings of the 2nd ACM international symposium on Mobile ad hoc networking & computing*. ACM, 2001, pp. 95–105.

[19] O. Bazan and M. Jaseemuddin, "On the design of opportunistic mac protocols for multihop wireless; networks with beamforming antennas," *IEEE Transactions on Mobile Computing*, vol. 10, no. 3, pp. 305–319, 2011.

[20] M. Yllmaz, M. Abdallah, H. El-Sallabi, J. Chamberland, K. Qaraqe, and H. Arslan, "Joint subcarrier and antenna state selection for cognitive heterogeneous networks with reconfigurable antennas," *Communications, IEEE Transactions on*, vol. 63, no. 11, Nov 2015.

[21] Y. Hou, M. Li, and K. Zeng, "Throughput optimization in multi-hop wireless networks with reconfigurable antennas," in *Computing, Networking and Communications (ICNC), 2017 International Conference on*. IEEE, 2017, pp. 620–626.

[22] P. Gupta and P. R. Kumar, "Critical power for asymptotic connectivity in wireless networks," in *Stochastic analysis, control, optimization and applications*. Springer, 1999, pp. 547–566.

[23] G. Nemhauser and L. Wolsey, "Integer and combinatorial optimization."

[24] J. Desrosiers, J. B. Gauthier, and M. E. Lübbecke, "Row-reduced column generation for degenerate master problems," *European Journal of Operational Research*, vol. 236, no. 2, pp. 453–460, 2014.

[25] Z. Li, E. Ahmed, A. M. Eltawil, and B. A. Cetiner, "A beam-steering reconfigurable antenna for wlan applications," *IEEE Transactions on Antennas and Propagation*, vol. 63, no. 1, pp. 24–32, 2015.

[26] G. L. Nemhauser and L. E. Trotter, "Vertex packings: structural properties and algorithms," *Mathematical Programming*, vol. 8, no. 1, pp. 232–248, 1975.